THE JOURNAL OF BIOLOGICAL CHEMISTRY
Vol. 279, No. 53, Issue of December 31, pp. 55801–55808, 2004
Printed in U.S.A.


# Thyroxine-Thyroid Hormone Receptor Interactions*

Received for publication, September 2, 2004
Published, JBC Papers in Press, October 4, 2004, DOI 10.1074/jbc.M410124200

**Ben Sandler‡, Paul Webb§, James W. Apriletti§, B. Russell Huber‡, Marie Togashi§, Suzana T. Cunha Lima§, Sanja Juric¶, Stefan Nilsson¶, Richard Wagner‡, Robert J. Fletterick‡, and John D. Baxter§‖**

*From the §Metabolic Research Unit and Diabetes Center and the ‡Departments of Biochemistry and Biophysics, University of California, San Francisco, California 94122 and ¶KaroBio AB, Novum S-141 57, Huddinge, Sweden*

**Thyroid hormone (TH) actions are mediated by nuclear receptors (TRs α and β) that bind triiodothyronine ($T_3$, 3,5,3′-triiodo-L-thyronine) with high affinity, and its precursor thyroxine ($T_4$, 3,5,3′,5′-tetraiodo-L-thyronine) with lower affinity. $T_4$ contains a bulky 5′ iodine group absent from $T_3$. Because $T_3$ is buried in the core of the ligand binding domain (LBD), we have predicted that TH analogues with 5′ substituents should fit poorly into the ligand binding pocket and perhaps behave as antagonists. We therefore examined how $T_4$ affects TR activity and conformation. We obtained several lines of evidence (ligand dissociation kinetics, migration on hydrophobic interaction columns, and non-denaturing gels) that TR-$T_4$ complexes adopt a conformation that differs from TR-$T_3$ complexes in solution. Nonetheless, $T_4$ behaves as an agonist *in vitro* (in effects on coregulator and DNA binding) and in cells, when conversion to $T_3$ does not contribute to agonist activity. We determined x-ray crystal structures of the TRβ LBD in complex with $T_3$ and $T_4$ at 2.5-Å and 3.1-Å resolution. Comparison of the structures reveals that TRβ accommodates $T_4$ through subtle alterations in the loop connecting helices 11 and 12 and amino acid side chains in the pocket, which, together, enlarge a niche that permits helix 12 to pack over the 5′ iodine and complete the coactivator binding surface. While $T_3$ is the major active TH, our results suggest that $T_4$ could activate nuclear TRs at appropriate concentrations. The ability of TR to adapt to the 5′ extension should be considered in TR ligand design.**

Thyroid hormone (TH)[1] plays important regulatory roles in metabolism, homeostasis, and development by binding and altering the transcriptional regulatory properties of two related nuclear receptors (NRs), the thyroid hormone receptors (TRs) α and β (1, 2). Most TH produced in the thyroid gland is secreted in the form of thyroxine ($T_4$; 3,5,3′,5′-tetraiodo-L-thyronine) (2, 3). The thyroid gland also produces smaller amounts of triiodothyronine ($T_3$; 3,5,3′-triiodo-L-thyronine) and reverse $T_3$ ($rT_3$; 3,3′,5′-triiodo-L-thyronine), and 80% of $T_4$ is converted to $T_3$ and $rT_3$ in peripheral tissues by two selenium deiodinases, which are tissue-specific (4). Current beliefs are that $T_3$ is the dominant active form of TH; $T_3$ binds the TRs with an affinity about 20–30 times higher than that of $T_4$ (5–9), and some studies suggest that $T_3$ is present at higher concentrations in the nucleus than $T_4$ (10, 11). Nonetheless, the question of whether $T_4$ is simply a prohormone or an active TH species is not completely resolved. $T_4$ exerts rapid nongenomic effects at several loci distinct from TRs (12). Moreover, saturating levels of $T_4$ activate transcription of TH-responsive genes in cell culture (see for example Ref. 5). Whereas it is possible that at least some of this activity is due to $T_3$ generated from $T_4$ in the cell, these results suggest that $T_4$ may act as a TR agonist. Normal concentrations of plasma-free $T_4$ are about 4–6-fold higher than those of $T_3$ (19 pmol/liter of $T_4$ *versus* 4.3 pmol/liter $T_3$) and intracellular $T_4$ and $T_3$ levels can differ because of variations in uptake and $T_4$ to $T_3$ conversion (3); thus, it is conceivable that intracellular $T_4$ in some context could occupy a significant fraction of nuclear TRs.

If $T_4$ does behave as an agonist, then it should bind to TR in a similar way to $T_3$ and induce conformational changes in the TR similar to those induced by $T_3$ (13, 14). $T_3$ interacts with the TR ligand binding domain (LBD), located in the receptor C terminus. The x-ray crystal structure of TRα or TRβ complexed with $T_3$ reveals that hormone is completely enclosed in a ligand binding pocket within the core of the LBD. It is thought that the enclosure is due to ligand-induced packing of the LBD C-terminal helix 12 (H12) against the LBD; a rearrangement that also disrupts the corepressor binding surface and completes the coactivator binding surface, leading to exchange of coregulators and influence on gene expression *in vivo* (15).

Unlike $T_3$, $T_4$ possesses a bulky iodine substituent at the 5′-position of the first thyronine ring. X-ray crystal structures have been determined for TR-LBDs complexed with several different high affinity agonists, including $T_3$, Dimit (3, 5-dimethyl-3′isopropyl-L-thyronine), and the TRβ-specific ligands GC-1 (3,5 dimethyl-4-(4-hydroxy-3′-isopropylbenzyl)-phenoxy acetic acid), and KB141 (3,5-dichloro-4-[(4-hydroxy-3-isopropylphenoxy)phenyl] acetic acid) (16–18). In each of these cases,

* This work was supported by Grants DK41842 and DK64148 (to J. D. B.) and DK58390 (to R. J. F) from the National Institutes of Health. The costs of publication of this article were defrayed in part by the payment of page charges. This article must therefore be hereby marked "*advertisement*" in accordance with 18 U.S.C. Section 1734 solely to indicate this fact.

*The atomic coordinates and structure factors (codes 1YOX and 1XZX) have been deposited in the Protein Data Bank, Research Collaboratory for Structural Bioinformatics, Rutgers University, New Brunswick, NJ (http://www.rcsb.org/).*

‖ Has proprietary interests in, and serves as a consultant and deputy director to Karo Bio AB, which has commercial interests in this area of research. To whom correspondence should be addressed: Metabolic Research Unit and Diabetes Center, University of California School of Medicine, HSW1210, 513, Parnassus Ave., San Francisco, CA 94122-0540. Tel.: 415-476-3166; Fax: 415-564-5813; E-mail: Jbaxter918@aol.com.

[1] The abbreviations used are: TH, thyroid hormone; LBD, ligand binding domain; TR, thyroid receptor; $T_3$, triiodothyronine (3,5,3′-triiodo-L-thyronine); $T_4$, thyroxine (3,5,3′,5′-tetraiodo-L-thyronine); R.m.s., root mean square; MIBRT, 3,5-dibromo-4-(3′isopropyl-4′-hydroxyphenoxy)benzoic acid); DIBRT, 3,5-dibromo-4-(3′,5′-diisopropyl-4′-hydroxyphenoxy)benzoic acid; HIC, hydrophobic interaction columns; Dimit, 3, 5-dimethyl-3′isopropyl-L-thyronine; NR, nuclear receptor.

the agonist contains a 5′ hydrogen group that lies close to the inner surface of H12. We therefore predicted that compounds with bulky side groups would perturb the folding of H12 against the body of the LBD and exploited this feature to create TR antagonists based on the notion that 5′ extensions would preclude appropriate H12 packing and coactivator binding (19–24). For example, addition of a 5′ isopropyl group, similar in size to an iodine group, to the agonist MIBRT (3,5-dibromo-4-(3′isopropyl-4′-hydroxyphenoxy)benzoic acid) creates the TR antagonist DIBRT (3,5-dibromo-4-(3′,5′-diisopropyl-4′-hydroxyphenoxy)benzoic acid) (22). Thus, it is conceivable that $T_4$, with a 5′ iodine extension, could even behave as an antagonist in some settings. Improved understanding of the way that the TRs adapt to the 5′ iodine group will be therefore important for understanding $T_4$ action and key principles of NR antagonist design.

In this study, we examine $T_4$ interactions with TR, the way that $T_4$ influences TR activity *in vitro* and in cells in culture and determined the x-ray crystal structure of TR in complex with $T_4$. We find that the TR-$T_4$ complex is less stable than the TR-$T_3$ complex, and that $T_4$-liganded TRs exhibit properties that are similar to unliganded TRs in solution. Nonetheless, $T_4$ behaves as an agonist in cell-free assays and transfected cells. The x-ray structure of the TR LBD-$T_4$ complex reveals that a previously undetected niche in the ligand binding pocket widens, relative to the size of the pocket observed in the TR$\beta$-$T_3$ complex, to accommodate the 5′ iodine, permitting H12 to pack against the LBD surface in the presence of the larger ligand. Thus, the enclosed TR hormone binding pocket accommodates $T_4$ without complete disruption of overall TR-LBD structure. These results suggest that $T_4$ will act largely as a TR agonist if present at high enough concentrations in the nucleus.

## MATERIALS AND METHODS

*Thyroid Hormone Binding Assay*—Thyroid hormone binding and analog competition assays were performed as previously described (9). $K_d$ values were calculated by fitting saturation curves and competition data to the equations of Swillens (25) using the GraphPad Prism program (GraphPad Software, San Diego, CA).

*Hydrophobic Interaction Chromatography of TR*—TR-LBDs were expressed in *E. coli* and partially purified on phenyl-Toyopearl, TSK-DEAE, TSK-heparin, and TSK-phenyl columns without TH as described previously (9). For each analog tested, TR was incubated for 1 h with a 5-fold molar excess of the analog relative to the final TR concentration, ammonium sulfate concentration was adjusted to 0.7 M, and the sample was loaded and chromatographed on a 0.8 × 7.5 cm TSK-phenyl column (Tosoh Biosep, Montgomeryville, PA) at 0.75 ml/min with a 60-min gradient from 0.7 M ammonium sulfate, no glycerol to no salt, 20% glycerol. TR levels were assessed by measuring absorption at 280 nM and, where appropriate, radiolabeled $T_4$ in complex with the TR was detected by scintillation.

*GST Pull-down Assay*—Labeled TRs were expressed using a TnT-coupled transcription translation kit. GRIP1 (amino acids 563–1121) (26), TRAP220-(622–701) (27), and N-CoR-(1944–2453) (28) were prepared in *Escherichia coli* BL21 as a fusion protein with glutathione *S*-transferase as per the manufacturer's protocol (Amersham Biosciences). Binding experiments were performed by mixing glutathione-linked Sepharose beads containing 4 $\mu$g of GST fusion proteins (Coomassie Plus protein assay reagent, Pierce) with 1–2 $\mu$l of $^{35}$S-labeled TR in 150 $\mu$l of binding buffer (20 mM HEPES, 150 mM KCl, 25 mM $MgCl_2$, 10% glycerol, 1 mM dithiothreitol, 0.2 mM phenylmethylsulfonyl fluoride, protease inhibitors, and 20 $\mu$g/ml bovine serum albumin) for 1.5 h. Beads were washed three times with 200 $\mu$l of binding buffer, and bound proteins were separated using 10% SDS-polyacrylamide gel electrophoresis and visualized by autoradiography.

*Electrophoretic Mobility Shift Assays—In vitro* translated TR was produced in reticulocyte lysates, TnT T7 Quick (Promega), and 20 fmols of translated receptor were incubated with 300,000 cpm of [$\gamma$-$^{32}$P]ATP-radiolabeled F2 oligonucleotides and 1 $\mu$g of poly(dI-dC) (Amersham Biosciences) in a 20-$\mu$l volume (29–31). The binding buffer contained 25 mM HEPES, 50 mM KCl, 1 mM dithiothreitol, 10 $\mu$M $ZnSO_4$, 0.1% Nonidet P-40, 5% glycerol. After 30 min at room temperature, the mixture was loaded onto a 5% nondenaturing polyacrylamide gel that was previously run for 30 min at 200 V. To separate TR-DNA complexes, the gel was run at 4 °C for 120–180 min at 200 V, using a running buffer containing 45 mM Tris borate (pH 8.0), and 1 mM EDTA.

*Reporter Cells*—The assay procedure, described previously (22), utilized Chinese hamster ovary cells stably expressing TR$\alpha$1 and TR$\beta$1 containing a stably integrated reporter gene with a single TRE (DR-4) cloned into the position of the mouse mammary tumor virus promoter hormone response element, driving expression of alkaline phosphatase coding sequences.

*Crystallization and Data Collection*—The TR$\beta$ LBD was purified for crystallization trials using cobalt affinity and hydrophobic interaction chromatography first without and then with hormone as previously described (18). Crystals of the $T_3$ complex were obtained by the hanging drop method, with a 10.5 mg/ml protein stock solution and mother liquor consisting of 100 mM sodium cacodylate and 900 mM sodium acetate, pH 7.2. Crystals were cryoprotected by immersion in sequential baths of 100 mM sodium cacodylate and 1.1 M sodium acetate, pH 7.2, with 3, 8, and 15% glycerol. Crystals were subjected to a final swipe through a bath with 25% glycerol before flash-freezing in liquid nitrogen.

Crystals of the $T_4$ complex were obtained similarly, with a crystallization mother liquor of 100 mM sodium cacodylate and 700 mM sodium acetate, pH 7.4. Use of extremely fresh protein and microseeding with Triac-hTR$\beta$ LBD crystals (< 0.1% of the final crystal) were found to be essential to obtaining diffraction quality crystals. Crystals were then cryoprotected using sequential glycerol baths as for the $T_3$ complex, but with a mother liquor of 100 mM sodium cacodylate and 900 mM sodium acetate, pH 7.4. Crystals were analyzed at the Advanced Light Source synchrotron facility, beamline 5.02. For the $T_3$ complex, 135° of data were collected with 1.5° oscillations; for the $T_4$ complex, 73° of data were collected with 0.5° oscillations. Reflections were indexed in DENZO and scaled in SCALEPACK.

*Structural Refinement of the $T_3$ Complex*—A molecular replacement solution was found using EPMR, employing the wild-type TR$\beta$/TRIAC structure with hormone omitted as a probe. The structure was then subjected to multiple rounds of simulated annealing, followed by positional and B-factor refinement in CNS. Occupancies were refined in CNS for arsenic atoms only. Refinement was then continued using REFMAC of the CCP4 suite. In the final stages of refinement, water molecules were added to the structure both manually and in ARP/wARP. Refinement steps alternated with manual rebuilding steps in Quanta98 and O, guided by $F_o - F_c$ and $2F_o - F_c$ maps calculated using FFT of the CCP4 suite, and a simulated annealing omit map calculated using CNS.

*Structural Refinement of the $T_4$ Complex*—The $T_4$ data set was subjected to molecular replacement in EPMR and simulated annealing and positional, B-factor, and occupancy refinement in CNS as for the $T_3$ complex. In light of the markedly higher resolution of the data for the $T_3$ complex, the refined $T_3$ structure was then least squares fitted in O to the model of the $T_4$ complex. A composite model consisting of protein from the fitted $T_3$ complex and ligand from the $T_4$ complex was created and used for subsequent refinement against the $T_4$ complex data.

To guard against model bias, this composite model was subjected to simulated annealing and positional refinement in CNS. However, this treatment raised $R_{free}$ markedly, as compared with $R_{free}$ of the composite after positional refinement only. This indicates that the true structure of the $T_4$ complex is close to the $T_3$ complex model used to create the composite. Subsequent refinement and model rebuilding were carried out as described above for the $T_3$ complex.

## RESULTS

*The TR-$T_4$ Complex Is Less Stable Than the TR-$T_3$ Complex and Adopts a Different Conformation in Solution*—We first investigated interactions of TRs with $T_3$ and $T_4$ (Fig. 1*A*). We previously determined that $T_3$ has an affinity for TRs ($K_d$ = 0.06 nM) about 30-fold higher than $T_4$ ($K_d$ = 2 nM) (6). $T_4$ also dissociates from TRs more rapidly than $T_3$ (Fig. 1, *B* and *C*). Whereas it took 8.4 and 6.2 h for half the $T_3$ to dissociate from *in vitro* translated preparations of TR$\alpha$ and TR$\beta$ at 4 °C, it only took about 0.15 h and 0.06 h for half of the $T_4$ to dissociate from TR$\alpha$ and TR$\beta$, respectively. Thus, TRs form a complex with $T_4$ that is significantly less stable than the TR-$T_3$ complex.

We next examined elution of $T_4$-liganded TRs from TSK-

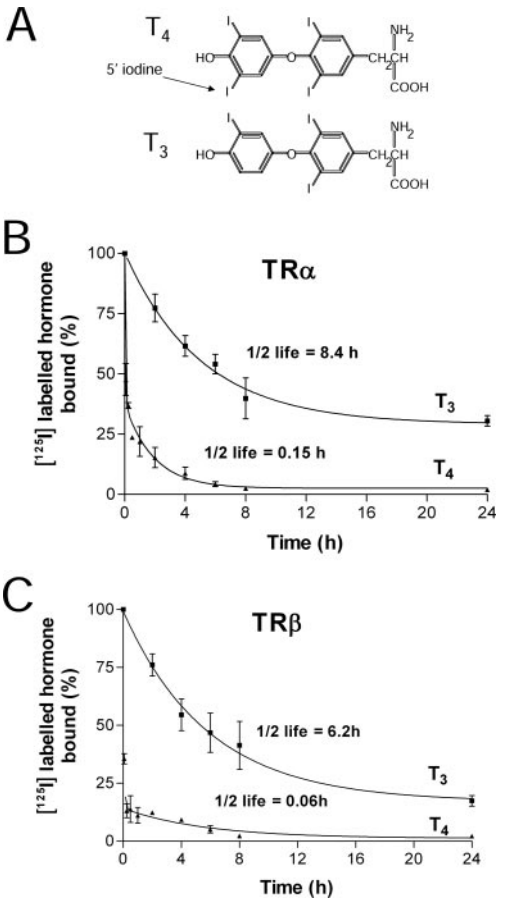


FIG. 1. **TR interactions with $T_3$ and $T_4$.** *A*, structures of $T_3$ and $T_4$ are presented with the iodine group at the 5′ position of the first thyronine ring *highlighted*. *B*, dissociation curves for $T_3$ and $T_4$ determined with the TR$\alpha$ LBD. *C*, as above, but determined with the TR$\beta$-LBD.

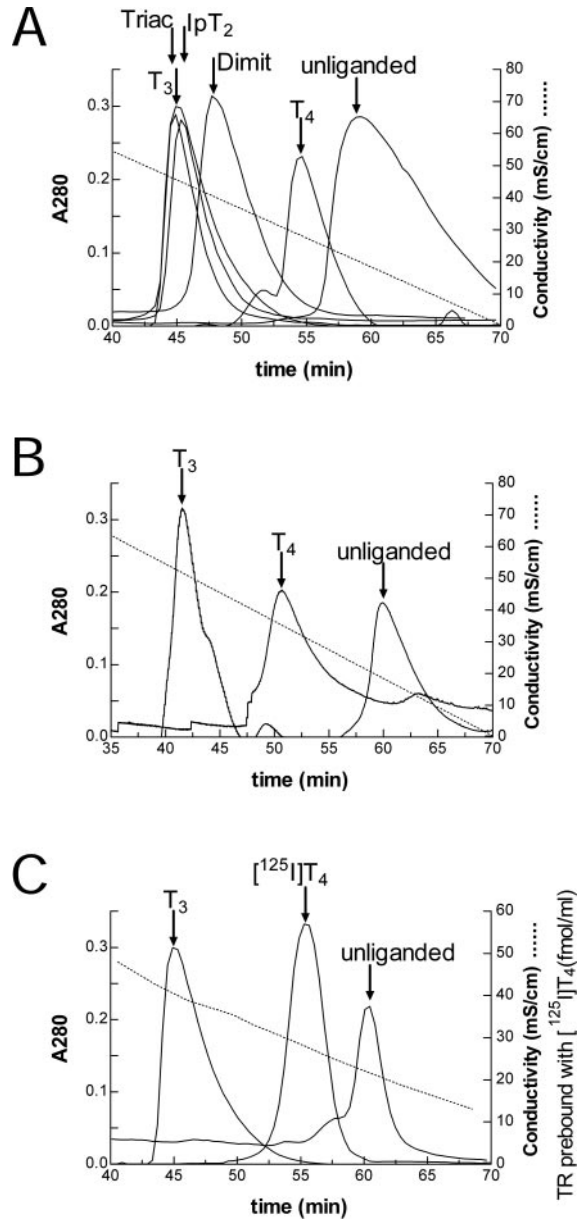


FIG. 2. **TR-$T_3$ and TR-$T_4$ complexes adopt different conformations.** *A*, elution profiles for purified TR$\alpha$ LBDs in complex with different agonist ligands or unliganded from hydrophobic interaction chromatography columns. *B*, as above, with TR$\beta$ LBD. *C*, as in *A*, with TRs bound to labeled $T_4$.

phenyl hydrophobic interaction columns (HIC), an assay that detects ligand-dependent conformational alterations in TR-LBDs and provides a crude index of hydrophobicity (9). In accordance with previous results (9), liganded TR$\alpha$-LBDs eluted ahead of unliganded TRs (Fig. 2*A*). Moreover, TR preparations in complex with several agonists $T_3$, Triac (3,3′,5′-triiodothyroacetic acid), 3′-Ip$T_2$ (3′-isopropyl-3,5-diiodo-L-thyronine), and Dimit eluted nearly together, with elution order paralleling relative affinities of ligand for TR ($T_3$ = Triac > Ip$T_2$ > Dimit). By contrast, the TR$\alpha$-$T_4$ complex eluted closer to unliganded TR. Similar results were also obtained with the TR$\beta$ LBD; the TR$\beta$-$T_4$ complex eluted from the column between the TR$\beta$-$T_3$ complex and unliganded TR$\beta$ (Fig. 2*B*).

It is unlikely that the unusual elution profile of the TR-$T_4$ complex is related to the low affinity of $T_4$ for TRs; the TR$\alpha$-Dimit complex eluted at a similar position to other TR agonist complexes even though Dimit binds TR$\alpha$ with an affinity five times lower than $T_4$ ($K_d$ = 9 nM for Dimit *versus* 2 nM for $T_4$). It is also unlikely that the unusual elution profile is related to rapid $T_4$ release during passage over HIC. Continuous dissociation of $T_4$ would lead to a broad curve and not a discrete symmetric peak as observed here, although the "shoulder" observed with the TR$\beta$-$T_4$ complex may reflect $T_4$ dissociation (Fig. 2*B*). Nonetheless, we directly examined migration of [$^{125}$I]$T_4$ prebound to TR$\alpha$ on HIC (Fig. 2*C*). Radiolabeled $T_4$ migrated at the same position as the TR$\alpha$-$T_4$ complex, whereas free $T_4$ did not elute from the column in these timescales (not shown), confirming that TR remains bound to $T_4$ as it passes over HIC. Thus, the unique elution profile of the TR-$T_4$ complex reflects an unusual conformation that exposes more hydrophobic surface than TRs in complex with $T_3$ or other analogues.

*Modulator Binding Properties of TR-$T_4$ Complexes Resemble Those of TR-$T_3$ Complexes*—We next determined whether $T_4$ behaved as an agonist under cell-free conditions. Fig. 3*A* shows that $T_4$ and $T_3$ promoted equivalent levels of TR binding to bacterially expressed nuclear receptor interacting regions of the coactivators GRIP1 and TRAP220. $T_4$ and $T_3$ also showed comparable activity in promoting binding of radiolabeled full-length GRIP1 and TRAP220 to bacterially expressed TR$\beta$-LBD (not shown). Finally, both ligands promoted TR release from bacterially expressed preparations of the receptor-interacting region (C terminus) of the corepressor, N-CoR (Fig. 3*B*). Thus, $T_4$ and $T_3$ behave as agonists in cell-free conditions.

TR agonists promote near complete dissociation of TR dimers, but not RXR-TR heterodimers, from DNA response

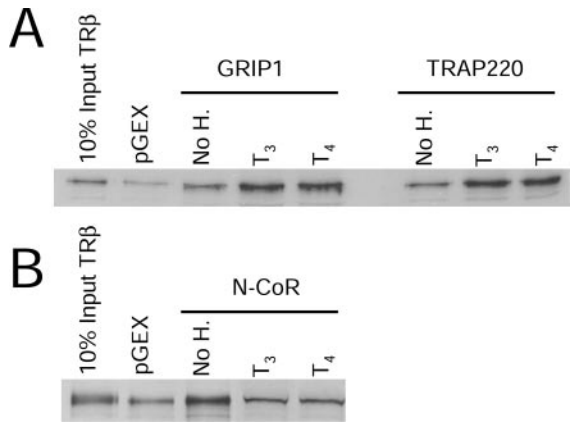


FIG. 3. **$T_4$ acts as an agonist *in vitro*.** *A*, autoradiograms of SDS-polyacrylamide gels, showing the amount of radiolabeled TR$\beta$ retained on columns containing bacterially expressed nuclear receptor-interacting fragments of GRIP1 and TRAP220. *B*, as in *A*, except that the NR-interacting region of the corepressor N-CoR is used as bait for TR.

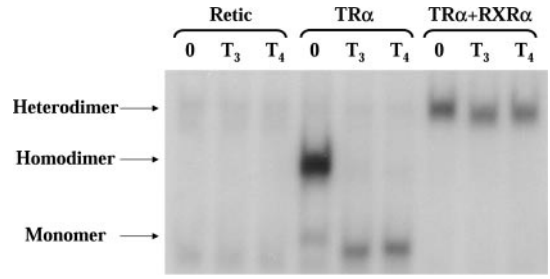


FIG. 4. **$T_4$ resembles $T_3$ in effects on TR DNA binding activities.** The figure shows an autoradiogram of an electrophoretic mobility shift assay to resolve a radiolabeled F2/IP-6 oligonucleotide in complex with hTR$\alpha$ or hTR$\alpha$/RXR$\alpha$ heterodimers (±) different forms of TH.

elements (TREs) containing half-sites aligned as inverted palindrome (F2/IP-6) or direct repeats (DR-4) (29, 30). $T_4$ and $T_3$ both promoted TR$\alpha$ homodimer release from an F2/IP-6 element and enhanced interactions of TR monomers with the same element (Fig. 4). Both forms of TH only modestly reduced RXR-TR$\alpha$ heterodimer binding in the same conditions. Similar results were also obtained using DR-4, and with TR$\beta$ and both TREs (not shown). Nonetheless, TR migration was slower in the presence of $T_4$ than $T_3$ (this was most evident for the monomer). Thus, $T_4$ resembles $T_3$ in terms of regulation of DNA binding activity, but TR-$T_4$ and TR-$T_3$ complexes exhibit different mobilities, underscoring the idea that TR-$T_4$ complexes adopt a different structure from TR-$T_3$ complexes in solution (see Fig. 2).

*$T_4$ Behaves as a TR Agonist in Cell Culture*—We next examined the behavior of $T_4$ in cell culture. $T_4$ elicited a similar maximal response to $T_3$ in cultured chinese hamster ovary cells that were stably transfected with a TH-regulated reporter gene and a vector that expresses either TR$\alpha$ (TRAF$\alpha$ cells, Fig. 5*A*) or TR$\beta$ (TRAF$\beta$ cells, Fig. 5*B*) (22, 32). In both cases $T_4$ exhibited a potency that is about 10% that of $T_3$. It is unlikely that $T_4$ to $T_3$ conversion accounts for the activity of administered $T_4$ in these conditions for several reasons. Treatment of TRAF cells with optimal doses of the deiodinase inhibitors iopanoic acid or propylthiouracil (PTU) did not alter the $T_3$ or $T_4$ dose response, and we did not detect significant $T_4$ to $T_3$ conversion assayed by high performance liquid chromatography of TRAF cell extracts (not shown). Moreover, spiking $T_4$ preparations with $T_3$ (to account for 10% of total TH on a molar basis) yielded a leftward shift in $EC_{50}$ relative to $T_4$ alone (Fig. 5*C*), suggesting that $T_4$ to $T_3$ conversion of 10% (and probably lower) can be detected in this system. Thus, $T_4$ behaves as a full agonist in cells in conditions in which conversion to $T_3$ is unlikely to contribute significantly to agonist activity.

*The X-ray Crystal Structure of the TR$\beta$-$T_4$ Complex Reveals That the LBD Adapts to the 5′-Iodine of $T_4$ and Completes the Coactivator Binding Surface*—To determine how TRs accommodate $T_4$ within the ligand binding pocket and perceive the compound as an agonist despite the presence of the bulky 5′ iodine group, we obtained structures of the TR$\beta$-LBD in complex with $T_3$ and $T_4$. Data collection and refinement statistics are presented in Table I. A ribbon diagram of the $T_4$-liganded TR$\beta$ structure (*pink*), superimposed over the $T_3$-liganded TR$\beta$ structure (*cyan*) is shown in Fig. 6. The complexes are similar in overall fold, both to each other and to previously determined structures of TR LBDs bound to agonists. Moreover, $T_4$ is completely buried within the core of the LBD, just like other agonists. The TR$\beta$-$T_3$ structure has a pocket volume of 572 Å$^3$, whereas the TR$\beta$-$T_4$ structure exhibits a pocket volume of 607 Å$^3$, as determined by GRASP (33). The TR$\beta$-$T_3$ and TR$\beta$-$T_4$ structures share the same space group and crystal contacts. Thus, differences in pocket volume between these two structures are probably attributable to the difference in the size of the ligand.

Direct comparisons of the TR-$T_4$ and TR-$T_3$ complexes (using "blinking" between aligned LBD structures in Insight II (Accelrys)) revealed concerted backbone shifts in four distinct regions. The first comprises H12, the H11-H12 loop and the wall of the ligand binding pocket and lies close to the 5′ iodine group (Fig. 6). The other regions include: N-terminal residues 199–212 (part of the DNA binding domain C-terminal helix (H0), which is included in this structure); H2 residues 234–243, portions of the underlying $\beta$-sheet (residues 318–321 and 325–339) and the loop between H2 and H3; and the N terminus of H3 (residues 248–267). Each of these regions of TR usually exhibits poor electron density in crystals, suggesting that they correspond to mobile regions of the protein (16–18). Thus, alterations in these regions are less likely to be significant for understanding ligand discrimination than those of H11-H12 region.

The H11-H12 loop (residues 445–453) is shifted by about 1 Å in the TR-$T_4$ structure relative to the TR-$T_3$ structure (Fig. 7), the C terminus of H11 (residues 437–444) is pulled inwards toward the pocket, accentuating a kink also present in the $T_3$ structure and other agonist-bound TR LBD structures, and the C-terminal end of H12 (residue 460) is pushed outwards in the presence of $T_4$. Despite these alterations, residues that comprise the coactivator binding surface (on H12 and the upper part of H3 and H5) adopt a structure with backbone positions identical to those seen in the TR-$T_3$ structure, and side chain positions nearly identical. This is consistent with the finding that $T_4$ promotes coactivator binding *in vitro*, and displays agonist activity *in vivo*. Nonetheless, direct comparisons in Rasmol indicate that H12 (residues 452–460) has closer contacts with the main body of the LBD in the $T_3$ complex than in the $T_4$ complex. This suggests that H12 packs less tightly against the LBD. Moreover, the average B-factor for protein atoms was higher for TR-$T_4$ (54.05) than for TR-$T_3$ (49.61), and the TR-$T_4$ structure had lower resolution (3.1 Å) than the TR-$T_3$ structure (2.5 Å). Thus, the TR$\beta$-$T_4$ complex exhibits a greater degree of disorder than the TR-$T_3$ structure.

The conformational alterations that occur within the hormone binding pocket near the $T_4$ 5′ iodine group are shown in detail in Figs. 8 and 9. Strikingly, the 5′ iodine fits neatly into a small "niche" in the wall of the pocket (Fig. 8*A*). This feature is analogous to similar niches that accommodate the other iodine groups in the $T_4$ and $T_3$ structures and is comprised of two distinct parts: an upper region that consists of residues

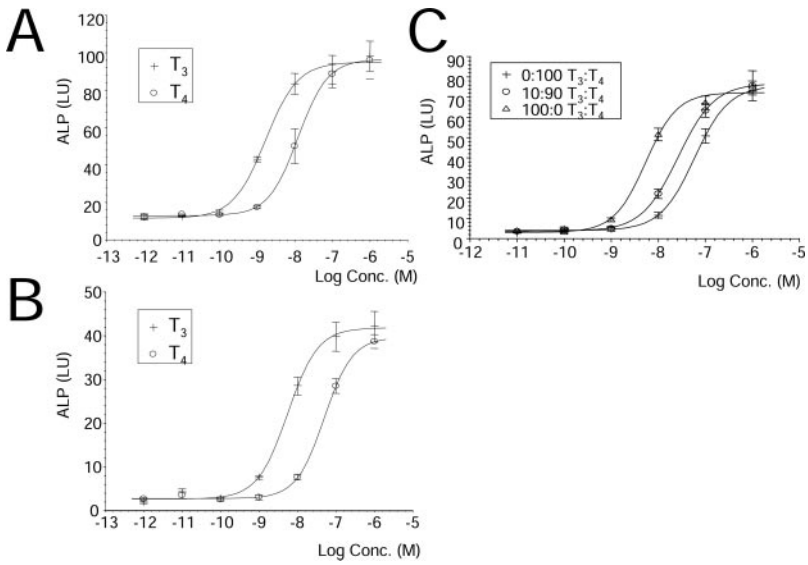


FIG. 5. **$T_4$ acts as an agonist in mammalian cell cultures.** *A*, graph shows alkaline phosphatase activity (the alkaline phosphatase gene is under control of a TH-regulated promoter) as a function TH concentration in chinese hamster ovary cells stably transfected with human TR$\alpha$ (TRAF-$\alpha$ cells). *B*, as in *A*, except that the experiment was performed in CHO cells stably transfected with TR$\beta$ (TRAF-$\beta$ cells). *C*, as in *A*, except that an additional treatment ($T_4$ preparations spiked with 10% $T_3$) was employed.

TABLE I
*Data collection and refinement statistics*

| | $T_3$ | $T_4$ |
|---|---|---|
| Data Collection | | |
| Spacegroup | P3121 | P3121 |
| Cell dimensions | | |
| *a*, *b* (Å) | 68.764 | 68.790 |
| *c* (Å) | 130.943 | 130.400 |
| Resolution (Å) | 2.5 | 3.1 |
| Reflections | 109,848 | 27,682 |
| Unique Reflections | 12,903 | 6,881 |
| Completeness | 99.7% | 99.4% |
| $R_{sym}$ (overall) | 0.08 | 0.07 |
| $R_{sym}$ (highest resolution shell) | 0.35 | 0.31 |
| Refinement | | |
| $R_{working}$ | 18.38 | 21.96 |
| $R_{free}$ | 24.32 | 26.12 |
| R.m.s. bond length (Å) | 0.031 | 0.040 |
| R.m.s. bond angle (°) | 2.310 | 2.780 |

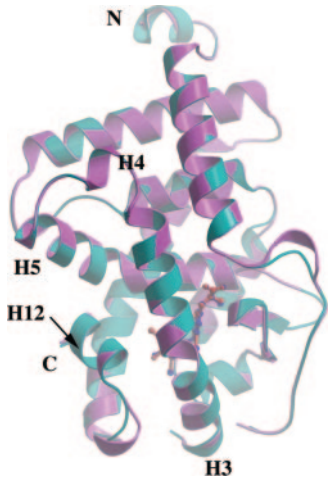


FIG. 6. **Structure of the TR$\beta$-$T_4$ complex.** Superimposed ribbon diagrams of TR$\beta$-$T_3$ complex (*cyan*) and the TR$\beta$-$T_4$ complex (*pink*) show that the overall fold is nearly identical. The coactivator binding surface H3, 4, 5, and 12 is labeled.

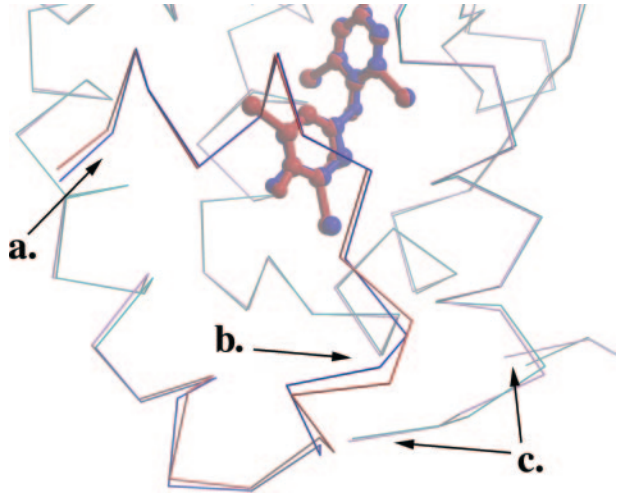


FIG. 7. **Superimposed views of the backbone trace of the TR$\beta$ H11-H12 region derived from TR$\beta$-$T_4$ and TR$\beta$-$T_3$ structures.** Backbone displacements in TR-$T_4$ (*red*) relative to TR-$T_3$ (*blue*). Helix 12 is *highlighted*. Displacements near the ligand binding pocket are confined to three areas: (*a*) C terminus of helix 12, (*b*) loop connecting helices 11 and 12, (*c*) disordered loop consisting of residues 250–265 linking nearby helices 2 and 3. Despite these structural alterations, the center of helix 12 shows no backbone displacement and completes the coactivator binding surface.

from several static helices that line the pocket of the LBD (Ile$^{276}$ on H3, and Met$^{310}$, Met$^{313}$ on H6), and a lower region comprised of His$^{435}$ on H11, and Phe$^{455}$ and Phe$^{459}$ on H12. This precisely positioned niche permits TR to accommodate $T_4$ completely within the enclosed pocket despite the presence of the 5′ iodine group. The niche is also present within the TR$\beta$-$T_3$ structure, but it is smaller (Fig. 8*B*). Superimposition of the TR-$T_4$ and TR-$T_3$ complexes reveals this region of the pocket expands slightly in the presence of $T_4$ (Fig. 9, compare *mesh surface*, $T_4$ with *solid surface*, $T_3$). This expansion is a result of a number of amino acid side chain shifts. The largest involves Met$^{310}$ (on H6), which lies above the 5′ iodine in the TR-$T_4$ complex. If one considers the receptor in the orientation seen in Fig. 9, a steric clash between Met$^{310}$ and the 5′-iodine shifts the entire ligand toward the "left" of the receptor relative to the position of ligand in the TR$\beta$-$T_3$ complex (detailed in Table II). This repositioning accentuates further steric clashes between the 5′ iodine group and side chains of two residues (Phe$^{455}$, Phe$^{459}$) on H12 itself. In addition, the kink in H11 probably results from a steric clash between the 5′ iodine and His$^{435}$ (see Table II for distances). These alterations enlarge the niche that accommodates the 5′ iodine substituent and permit H12 to pack against the LBD and complete the coactivator binding surface.

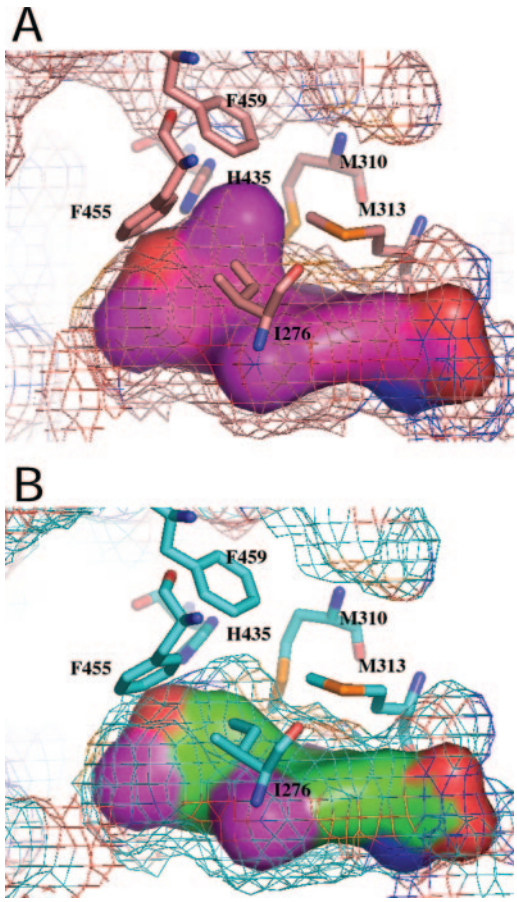


FIG. 8. **Comparison of the architecture of the TR ligand binding pocket in the presence of different ligands.** *A* and *B*, close-up view of the ligand binding pocket with side chains of the residues lining the niche, which accommodates the 5′ iodine group. Inner surfaces of the pockets are shown as *mesh contours*, whereas surfaces of the ligands are shown as *solid contours*. *A*, pocket of the TR-$T_4$ complex. *B*, pocket of the TR-$T_3$ complex. The figures were created in PyMol (pymol.sourceforge.net/).

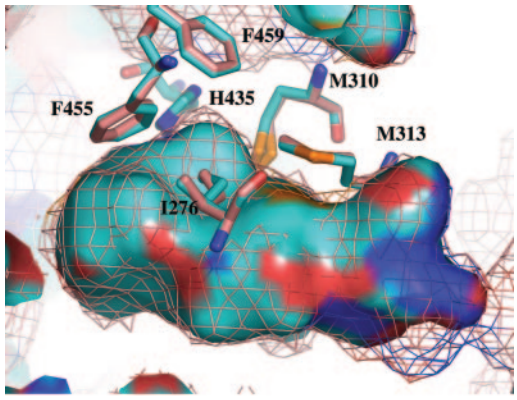


FIG. 9. **Structural alterations in the ligand binding pocket that permit TR$\beta$ to accommodate $T_4$.** Superimposed images of the side chains and pockets of $T_4$ (*pink bonds*, *mesh surface*)- and $T_3$- (*cyan bonds*, *solid surface*) liganded TRs.

## DISCUSSION

The current studies address $T_4$ interactions with TRs. As developed in the Introduction, $T_3$ is thought to be the major active form of TH and binds TRs with ~30-fold the affinity of $T_4$ (6). Free circulating $T_4$ levels are, however, about four to six times that of $T_3$ and intracellular $T_4$/$T_3$ ratios can vary, so it is conceivable that $T_4$ could occupy a significant fraction of nuclear TRs in some contexts. The lower affinity of $T_4$ for TRs is probably related to the bulky 5′-iodine moiety that, based on our previous structures of TR-LBDs in complex with $T_3$ and related agonists, should not fit readily into the hormone binding pocket (14, 16–18). Indeed, placement of some bulky 5′ extensions on high affinity TR agonists can even create antagonists (21). Thus, we asked how $T_4$ interacts with TR, whether it behaves as an agonist or antagonist, and how it can fit into the TR ligand binding pocket.

TABLE II
*Table of neighbor atoms*

Distances between the 5′ iodine of $T_4$ and neighbor atoms, defined as atoms within 4 Å. Hypothetical distances are measured between the $T_4$ iodine and side chain atoms of the TR$\beta$ -$T_3$ structure, least-squares fitted to the TR$\beta$ -$T_4$ structure in Insight II.

| Residue | Real (Å) | Hypothetical | Shift |
|---|---|---|---|
| $Met^{310}$ CE | 3.85 | 3.29 | +0.56 |
| $Ile^{276}$ CD1 | 3.66 | 3.29 | +0.37 |
| $Phe^{455}$ CE1 | 3.98 | 3.76 | +0.22 |
| $Phe^{459}$ CE1 | 3.57 | 3.41 | +0.16 |
| $His^{435}$ CE1 | 3.18 | 3.08 | +0.10 |
| $His^{435}$ NE1 | 3.23 | 3.35 | −0.12 |
| $Met^{313}$ CE | 3.12 | 3.11 | +0.01 |

We initially examined properties of TR-$T_4$ complexes. We confirmed that $T_4$ bound to TR more weakly than $T_3$, and further demonstrated that $T_4$ dissociates from TRs faster than $T_3$, (Fig. 1). Moreover, the TR complex with $T_4$ is less compact than that with $T_3$, as suggested by migration of TR-$T_4$ complexes closer to unliganded TRs than to TR-agonist complexes on HIC (Fig. 2, *A* and *B*) and in gel shift assays with DNA (Fig. 4). The unusual HIC elution profile is not a reflection of lower affinity of TR for $T_4$, because TR complexes with Dimit (which lacks a 5′ substituent yet only exhibits 20% of the affinity of $T_4$ for TR) elute at a similar position to TR-$T_3$ complexes (Fig. 2). It is also unlikely to reflect rapid dissociation of $T_4$ while on the column, because TRs in complex with radiolabeled $T_4$ also elute at a similar position to TRs in complex with unlabeled $T_4$ (Fig. 2*C*). Despite the less compact nature of the TR-$T_4$ complex, maximally effective doses of $T_4$ were as effective as those of $T_3$ in stimulating association of coactivators (GRIP1 and TRAP220; Fig. 3), release of corepressors (N-CoR and SMRT; Fig. 3) and dissociation of TR homodimers from DNA (Fig. 4). Moreover, maximally effective doses of $T_4$ were as effective as those of $T_3$ in stimulating activity of a TRE-regulated reporter in cultured cells that express TR$\alpha$ or TR$\beta$, and did so in conditions in which it is unlikely that agonist activity of $T_4$ stems from contaminating $T_3$ or intracellular conversion of $T_4$ to $T_3$. Thus, it is likely that $T_4$ and $T_3$ promote similar overall conformational rearrangements within the TR-LBD in these conditions and that H12 must fold into the active conformation in the presence of $T_4$.

The crystal structure of the TR$\beta$-$T_4$ complex supports the notion that $T_4$ induces a TR conformation similar to that observed with higher affinity agonists (Fig. 6). TR adopts this fold because, overall, $T_4$ fits tightly into the ligand binding pocket despite the presence of the 5′ iodine group. The pocket accommodates the bulky 5′ iodine via shifts in the position of several amino acid side chains in the pocket relative to their positions in the TR-$T_3$ complex. These changes enlarge a niche that lies close to the 5′-position of the first thyronine ring and closely matches the size and shape of the 5′ iodine (Figs. 8 and 9). The requirements for these structural alterations for fitting of $T_4$ relative to $T_3$ likely explain the reduced affinity of the TRs for $T_4$ relative to $T_3$. However, the niche permits H12 to fold over the bulky iodine group and complete the coactivator binding surface. Thus, the presence of an adaptable niche in the TR ligand binding pocket allows $T_4$ to behave as agonist, despite the 5′-extension.

Although H12 adopts the typical active conformation in the presence of $T_4$, our crystal structures indicate that the H11-H12 loop is more mobile and more loosely packed against the LBD in the presence of $T_4$ than in the presence of $T_3$ (Figs. 6 and 7). These features suggest explanations for the observed differences between the behavior of TR-$T_4$ and TR-$T_3$ complexes. A tendency of H12 to oscillate between conformations that resemble liganded and unliganded states would reduce the efficiency of the capping of the pocket and allow $T_4$ to dissociate more readily. Loose packing of H12 would also expose more of the hydrophobic interior of the protein, explaining unusual mobilities of the TR-$T_4$ complex in HIC and gel shifts. While $T_4$ consistently behaves as a full agonist in our hands, it is conceivable that the loose packing of H12 induced by $T_4$ *versus* $T_3$ could leave the TR open to external influences that alter the response to the ligand. For example, in cells with high corepressor and/or low coactivator levels, H12 might be forced into the unliganded conformation and $T_4$ could display partial agonist, or even antagonist, activity. This issue will require further investigation.

We do not yet have a similar structure of TR$\alpha$ in complex with $T_4$, but there are great overall similarities between the TR isoforms in terms of overall LBD fold (18), sequence and, as reported here, activity in the presence of $T_4$ and $T_3$ (Figs. 1, 2, and 5) suggesting that TR$\alpha$ will adapt to the 5′ iodine extension in a similar way to TR$\beta$. Interestingly, $T_4$ dissociates from TR$\beta$ even more rapidly than from TR$\alpha$ (Fig. 1). In this regard, TR$\beta$ tends to exhibit less rigidity in the vicinity of the H11-H12 region than equivalent structures of TR$\alpha$ in complex with the same ligand (as judged by temperature factors) (18). These differences in rigidity within the TR H11-H12 region may explain the increased dissociation rate of $T_4$.

We previously proposed that TR ligands with bulky 5′ side chains should perturb H12 and act as antagonists (reviewed in Ref. 21). This idea, the extension hypothesis (19, 20), has been partly validated by our synthesis of novel TR antagonists based on these principles (22–24), and structures of other NRs in complex with antagonists (such as selective estrogen receptor modulators) (34, 35). Nonetheless, $T_4$ acts as an agonist, just as we have learned that many other TR ligands with extensions that are even bulkier than the $T_4$ 5′ iodine group can behave as agonists (23, 24). Thus, the nature of the extension and its relationship to the rest of the ligand is important for overall agonist/antagonist activity, and TR must accommodate larger ligands in ways that cannot be easily predicted from structures of TR ligands without "extensions."

NR antagonists perturb H12 position in two ways, by directly interfering with H12 packing or occupying the pocket without inducing the structural changes required for the agonist configuration (reviewed in Ref. 21 and references therein). Our studies add to an emerging pattern, which suggests that NRs alter their conformations in a variety of ways to accommodate hormone analogs and allow them to act as agonists. The TR-$T_4$ crystal structure reported here reveals that the pocket can reorganize to accommodate the 5′ iodine group, but with a resulting strain of the overall structure relative to $T_3$. An extreme case of accommodation is for PXR, where the pocket expands to accommodate larger ligands and collapses to accommodate smaller ligands (36–38). In this case, packing does not appear to result in the stability differences we have detected between $T_4$- *versus* $T_3$-liganded TRs. Finally, we recently showed that TR accommodates a ligand (GC-24) that binds TR$\beta$ with about 40-fold the affinity of TR$\alpha$, and has a 3′ phenyl extension and a 5′ hydrogen (39), by opening up a hydrophobic patch on the inner surfaces of H3 and H11 that is not normally part of the pocket. It will be interesting to determine how TR accommodates ligands with even bulkier 5′ extensions (22–24), or why ligands with particular 5′ extensions, such as the DIBRT isopropyl group and the $NH_3$ phenyl group, act as antagonists.

Our studies do not address the question of whether $T_4$ is a relevant species of TH in physiological settings. As indicated in the Introduction, many factors regulate relative $T_4/T_3$ concentrations in the nucleus, making it difficult to gauge the extent to which intracellular $T_4$ participates in TR binding. Nonetheless, the observation that TR can reorganize to create a niche that precisely accommodates the $T_4$ 5′ iodine, coupled with the fact that the potency of $T_4$ is about 10% that of $T_3$ in cell culture and that free circulating $T_4$ concentrations are 4–6-fold those of $T_3$, raises the distinct possibility that $T_4$ could exhibit significant agonist activity in humans.

REFERENCES


1. Zhang, J., and Lazar, M. A. (2000) *Annu. Rev. Physiol.* **62,** 439–466
2. Yen, P. M. (2001) *Physiol. Rev.* **81,** 1097–1142
3. Braverman, L. E., and Utiger, R. D. (eds) (2000) *Werner's and Ingbar's The Thyroid: A Fundamental and Clinical Text*, 8th Ed., Lippincott Williams & Wilkins, Philadelphia, PA
4. Kohrle, J. (1999) *Mol. Cell. Endocrinol.* **151,** 103–119
5. Samuels, H. H., Stanley, F., and Casanova, J. (1979) *J. Clin. Investig.* **63,** 1229–1240
6. Apriletti, J. W., Eberhardt, N. L., Latham, K. R., and Baxter, J. D. (1981) *J. Biol. Chem.* **256,** 12094–12101
7. Ichikawa, K., DeGroot, L. J., Refetoff, S., Horwitz, A. L., and Pollak, E. R. (1986) *Metabolism* **35,** 861–868
8. Schueler, P. A., Schwartz, H. L., Strait, K. A., Mariash, C. N., and Oppenheimer, J. H. (1990) *Mol. Endocrinol.* **4,** 227–234
9. Apriletti, J. W., Baxter, J. D., Lau, K. H., and West, B. L. (1995) *Protein Expr. Purif.* **6,** 363–370
10. Surks, M. I., and Oppenheimer, J. H. (1977) *J. Clin. Investig.* **60,** 555–562
11. Silva, J. E., and Larsen, P. R. (1978) *J. Clin. Investig.* **61,** 1247–1259
12. Davis, P. J., Tillmann, H. C., Davis, F. B., and Wehling, M. (2002) *J. Endocrinol. Investig.* **25,** 377–388
13. Weatherman, R. V., Fletterick, R. J., and Scanlan, T. S. (1999) *Annu. Rev. Biochem.* **68,** 559–581
14. Ribeiro, R. C., Apriletti, J. W., Wagner, R. L., Feng, W., Kushner, P. J., Nilsson, S., Scanlan, T. S., West, B. L., Fletterick, R. J., and Baxter, J. D. (1998) *J. Steroid. Biochem. Mol. Biol.* **65,** 133–141
15. Glass, C. K., and Rosenfeld, M. G. (2000) *Genes Dev.* **14,** 121–141
16. Wagner, R. L., Apriletti, J. W., McGrath, M. E., West, B. L., Baxter, J. D., and Fletterick, R. J. (1995) *Nature* **378,** 690–697
17. Darimont, B. D., Wagner, R. L., Apriletti, J. W., Stallcup, M. R., Kushner, P. J., Baxter, J. D., Fletterick, R. J., and Yamamoto, K. R. (1998) *Genes Dev.* **12,** 3343–3356
18. Wagner, R. L., Huber, B. R., Shiau, A. K., Kelly, A., Cunha Lima, S. T., Scanlan, T. S., Apriletti, J. W., Baxter, J. D., West, B. L., and Fletterick, R. J. (2001) *Mol. Endocrinol.* **15,** 398–410
19. Scanlan, T. S., Baxter, J. D., Fletterick, R. J., Kushner, P., Wagner, R., Apriletti, J., West, B., and Shiau, A. (1996) University of California, International Patent
20. Ribeiro, R. C. J., Apriletti, J. W., Wagner, R. L., West, B. L., Feng, W., Huber, R., Kushner, P. J., Nilsson, S., Scanlan, T. S., Fletterick, R. J., Schaufele, F., and Baxter, J. D. (1998) *Recent Prog. Horm. Res.* **53,** 351–394
21. Webb, P., Nguyen, N. H., Chiellini, G., Yoshihara, H. A., Cunha Lima, S. T., Apriletti, J. W., Ribeiro, R. C., Marimuthu, A., West, B. L., Goede, P., Mellstrom, K., Nilsson, S., Kushner, P. J., Fletterick, R. J., Scanlan, T. S., and Baxter, J. D. (2002) *J. Steroid. Biochem. Mol. Biol.* **83,** 59–73
22. Baxter, J. D., Goede, P., Apriletti, J. W., West, B. L., Feng, W., Mellstrom, K., Fletterick, R. J., Wagner, R. L., Kushner, P. J., Ribeiro, R. C. J., Webb, P., Scanlan, T. S., and Nilsson, S. (2002) *Endocrinology* **143,** 517–524
23. Chiellini, G., Nguyen, N. H., Apriletti, J. W., Baxter, J. D., and Scanlan, T. S. (2002) *Bioorg. Med. Chem.* **10,** 333–346
24. Nguyen, N. H., Apriletti, J. W., Cunha Lima, S. T., Webb, P., Baxter, J. D., and Scanlan, T. S. (2002) *J. Med. Chem.* **45,** 3310–3320
25. Swillens, S. (1995) *Mol. Pharmacol.* **47,** 1197–1203
26. Ding, X. F., Anderson, C. M., Ma, H., Hong, H., Uht, R. M., Kushner, P. J., and Stallcup, M. R. (1998) *Mol. Endocrinol.* **12,** 302–313
27. Yuan, C. X., Ito, M., Fondell, J. D., Fu, Z. Y., and Roeder, R. G. (1998) *Proc. Natl. Acad. Sci. U. S. A.* **95,** 7939–7944
28. Hu, X., and Lazar, M. A. (1999) *Nature* **402,** 93–96
29. Ribeiro, R. C., Kushner, P. J., Apriletti, J. W., West, B. L., and Baxter, J. D. (1992) *Mol. Endocrinol.* **6,** 1142–1152
30. Ribeiro, R. C., Apriletti, J. W., Yen, P. M., Chin, W. W., and Baxter, J. D. (1994) *Endocrinology* **135,** 2076–2085
31. Ribeiro, R. C., Feng, W., Wagner, R. L., Costa, C. H., Pereira, A. C., Apriletti, J. W., Fletterick, R. J., and Baxter, J. D. (2001) *J. Biol. Chem.* **276,** 14987–14995
32. Ye, L., Li, Y. L., Mellstrom, K., Mellin, C., Bladh, L. G., Koehler, K., Garg, N., Garcia Collazo, A. M., Litten, C., Husman, B., Persson, K., Ljunggren, J., Grover, G., Sleph, P. G., George, R., and Malm, J. (2003) *J. Med. Chem.* **46,** 1580–1588
33. Nicholls, A., Sharp, K. A., and Honig, B. (1991) *Proteins* **11,** 281–296

34. Shiau, A. K., Barstad, D., Loria, P. M., Cheng, L., Kushner, P. J., Agard, D. A., and Greene, G. L. (1998) *Cell* **95,** 927–937
35. Brzozowski, A. M., Pike, A. C., Dauter, Z., Hubbard, R. E., Bonn, T., Engstrom, O., Ohman, L., Greene, G. L., Gustafsson, J. A., and Carlquist, M. (1997) *Nature* **389,** 753–758
36. Watkins, R. E., Davis-Searles, P. R., Lambert, M. H., and Redinbo, M. R. (2003) *J. Mol. Biol.* **331,** 815–828
37. Watkins, R. E., Maglich, J. M., Moore, L. B., Wisely, G. B., Noble, S. M., Davis-Searles, P. R., Lambert, M. H., Kliewer, S. A., and Redinbo, M. R. (2003) *Biochemistry* **42,** 1430–1438
38. Watkins, R. E., Wisely, G. B., Moore, L. B., Collins, J. L., Lambert, M. H., Williams, S. P., Willson, T. M., Kliewer, S. A., and Redinbo, M. R. (2001) *Science* **292,** 2329–2333
39. Borngraeber, S., Budny, M. J., Chiellini, G., Cunha-Lima, S. T., Togashi, M., Webb, P., Baxter, J. D., Scanlan, T. S., and Fletterick, R. J. (2003) *Proc. Natl. Acad. Sci. U. S. A.* **100,** 15358–15363